Combining structural data with monitoring data in open pit mines to interpret the failure mechanism and calibrate radar alarms

P Farina *Geoapp s.r.l., Italy*

F Bardi *Geoapp s.r.l., Italy*

L Lombardi *Università degli Studi di Firenze, Italy*

G Gigli *Università degli Studi di Firenze, Italy*

Abstract

In a moderately jointed rock mass, slope failure is generally defined by the presence and orientation of discontinuities that act as planes of weakness within the rock mass, thus controlling the size and the direction of ground movement. For this reason, when dealing with structurally-controlled slope movements, a method to support the interpretation of monitoring data could be to combine displacement records with structural data, especially when the monitoring system relies on radar. Since movement measurements provided by radar are line-of-sight (LOS), thus providing only magnitudes but not directions of slope displacement, they cannot be used for understanding the 3D failure kinematics and the corresponding behaviour. This poses a challenge in the interpretation of the deformation data provided by the radar and in the set-up of alarm thresholds that commonly assume that monitoring data provides true (total vector) movement, which could be significantly different from that measured by radar. In order to reconcile the directional component of radar measurements with actual movement, the authors investigated the use of kinematic analyses to interpret true movement from LOS data. An evolution of the kinematic analysis process was introduced with the concept of the 'kinematic hazard index' for each instability mechanism. Based on such a concept, it is possible to obtain maps of the relative probability of each of the different failure modes (plane failure, wedge, direct toppling, flexural toppling, and rockfall). The kinematic maps can become an essential input for the interpretation of radar data, allowing the slope engineer to associate measured ground movements with a possible failure mechanism. Moreover, from the kinematic maps, it is possible to derive the most likely direction of movement of each kinematic block, thus enabling the estimation of the sensitivity to movement measured by radar to an estimation of true movement for each sector of the pit. As a consequence, kinematic maps can also be used to refine the radar alarm thresholds by correcting the LOS measurements with respect to their sensitivity to the expected direction of movement. Within the framework of a research project funded by the LOPII, a methodology to implement the above described approach aimed at calibrating the radar alarms and at supporting the interpretation of radar alarms was developed and tested in a few selected mine sites owned by LOPII sponsors, where structurally controlled slope movements at different spatial scales represent a common issue and where slope monitoring radar units and robotic total stations were already deployed. The proposed and tested approach represents an operational methodology to support the understanding of the relationship between observed deformations and structural stability controls. In addition, the output of the analysis is aimed at improving the effectiveness of the slope monitoring program thanks to the input provided to a better selection of alarm thresholds.

Keywords: *kinematic analysis, slope stability radar, displacement direction, open pit mine*

1 Introduction

Kinematic analysis is a well-known method that is able to establish, through a graphical analysis of the rock block behaviour under its weight and only considering frictional shear strength along the discontinuity faces

Combining structural data with monitoring data in open pit mines to interpret
the failure mechanism and calibrate radar alarms

P Farina et al.

(no cohesion), if and where a particular instability mechanism is kinematically feasible, given the geometry of the slope and discontinuities present in the analysed sector of the slope (Goodman & Bray 1976; Hoek & Bray 1981; Matheson 1983; Hudson & Harrison 1997). In order to identify areas prone to fail on a new excavated bench face, an analysis of the kinematic admissibility to potential wedges or planes that intersect the excavation face is typically recommended. Kinematic analyses are in fact useful for the first definition of the susceptibility for the main mechanisms of instability, especially those present at bench or multi-bench scale. These are identified by combining fracture orientation with local slope orientation and frictional angles of the discontinuities and of their intersections. The instability mechanisms investigated with this approach are planar failure, wedge failure, block toppling and flexural toppling. An evolution of the kinematic analysis process was proposed by Casagli & Pini (1993) with the introduction of the 'kinematic hazard index' concept. The kinematic hazard index, ranging from 0 to 1 (0 if out of all the discontinuities none of them is able to satisfy the kinematic conditions for the analysed failure mechanism, 1 when all the discontinuities satisfy the kinematic conditions for the analysed mechanism), provide a qualitative estimation of the most likely mechanism potentially occurring in the analysed sector of the slope.

In the last years, the authors applied the concept of the kinematic hazard index, by analysing point clouds acquired by terrestrial laser scanners or photogrammetric systems through the use of specific algorithms included in the DiANA code (Gigli & Casagli 2011). The code is able to manage a great number of discontinuities with different friction angles, to calculate intersection lines automatically, together with the equivalent friction angle of the intersecting planes and the shape of the wedge and, finally, to generate maps of the kinematic index with the index calculated for each point of the cloud. Such a method has been called '3D kinematic analysis'. The obtained maps–one for each considered failure mechanism–show for each point of the cloud the relative probability of having that specific failure mode.

The knowledge of the most likely mechanisms potentially able to occur on the slope clearly represents an important support for the geotechnical engineers onsite, while analysing and interpreting radar data. Furthermore, by knowing which failure mechanism can be expected in the different sectors of the pit and the orientation of the discontinuity or the intersection between discontinuities controlling those mechanisms, it is possible to estimate the most likely direction of movement to be expected. By calculating the angle between the direction of the radar line-of-sight (LOS) and the expected direction of the movement, it is possible to estimate the sensitivity of the radar to the direction of movement and thus defining a 'correction factor' to calibrate the radar alarms.

Within the framework of a research project funded by the LOPII, a methodology to implement the above described approach–that was aimed at calibrating the radar alarms and at supporting the interpretation of radar alarms–was developed and tested in a few selected mine sites owned by LOPII sponsors, where structurally controlled slope movements at different spatial scales represent a common issue and where slope monitoring radar units and robotic total stations were already deployed. In Figure 1, a flow chart describing the above-mentioned procedure is shown. The proposed approach is based on the use, as input data, of laser scanner or photogrammetric point clouds, radar data and prism data. The main outputs of the methodology are represented by 3D kinematic maps, the map of the predominant mechanism, the radar sensitivity map and the calibrated radar alarms. The proposed methodology also includes a validation step, based on the comparison between the corrected displacement values obtained from the sensitivity of the radar to the estimated direction of movement and the 3D displacement values recorded onsite by total station (prisms data).
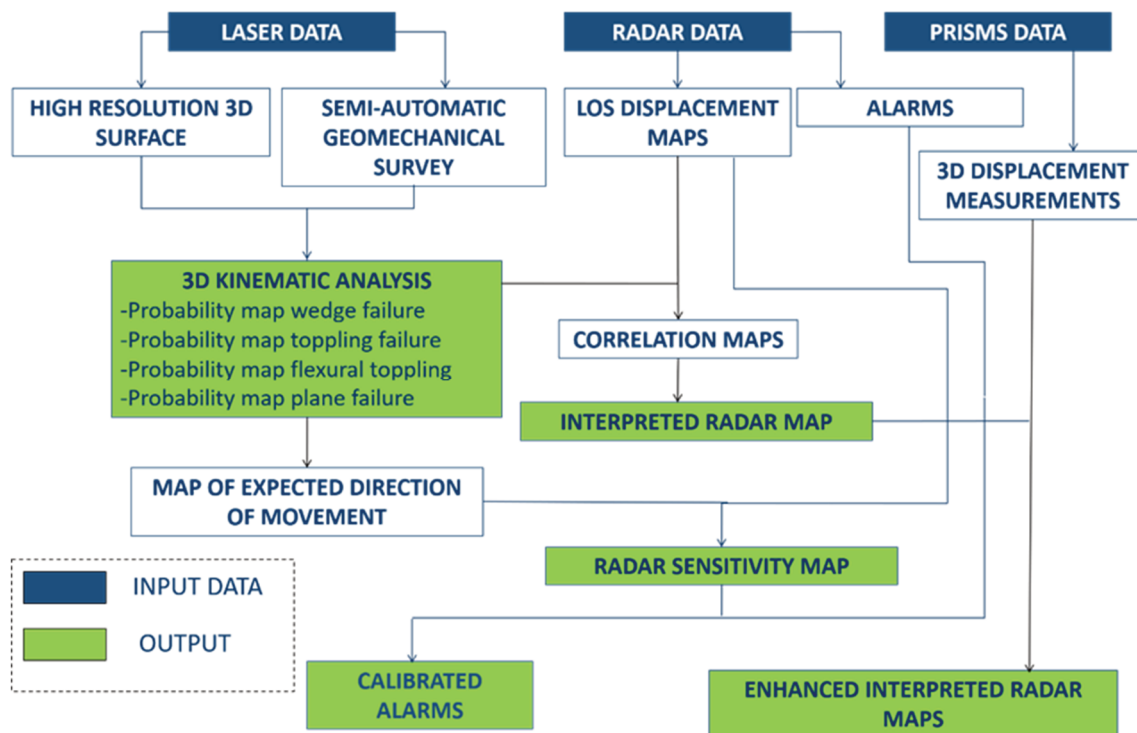
Figure 1 Flow chart of the proposed methodology showing in blue colour the input data and in green colour the outputs

The outcomes of the implementation of such a methodology in an open pit mine selected as test site, carried out in the framework of the LOPII research project, are briefly discussed in this paper.

The selected pit represents an interesting target for the proposed research activity, as it is affected by structurally controlled instabilities. It is also covered by an exhaustive slope monitoring system, including a slope stability radar and a robotic total station.

The first step of the project has been focused on the collection of the available data from the test site and on the acquisition of high-resolution point clouds of the pit to apply the proposed procedure.

2 Data collection

The technical staff of the test site provided fundamental information that was useful to apply the proposed methodology. Specifically, a topographic map of the area of interest has been provided to the scope of the research, together with the location and volume of past slope failures. This information allowed the authors to define the sector of interest within the pit.

The failures affecting this sector have also been monitored both by slope stability radar and total station, whose data have been made available to the scope of this project.

Some structural data (discontinuity sets, geotechnical domains, large structures) identified by photogrammetry have also been made available to this research and later compared with the results of the present study.

Moreover, in order to obtain high-resolution 3D point clouds that are characterised by centimetric accuracy, a Riegl VZ-1000 terrestrial laser scanner has been employed (Figure 2). The device is able to acquire the position of thousands of points per second from a maximum distance of 1,440 m, a maximum angular resolution of 0.0005°, and accuracy of 5 mm (one σ at 100-m range under RIEGL VZ-1000). The acquisition campaign has been performed from eight stations and employing 30 reflectors. The correct localisation of both the reflectors and the stations–performed by employing a differential GPS–represented a crucial step to correctly georeferencing the obtained point clouds. From each of the eight stations, high-resolution

Combining structural data with monitoring data in open pit mines to interpret
the failure mechanism and calibrate radar alarms

P Farina et al.

acquisitions have been performed and merged, obtaining a point cloud of the whole pit with a very high level of detail (average distance between points ranging between 1 and 3 cm) (Figure 3).

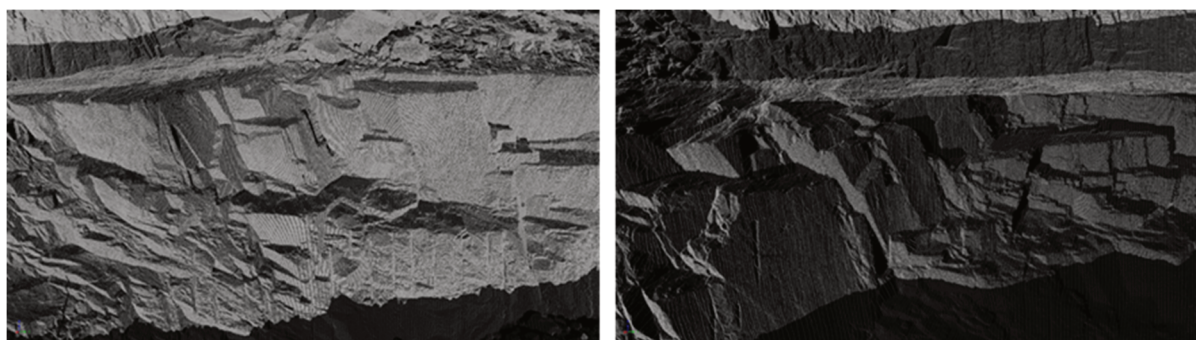**Figure 2**   Laser scanner survey done on a wall of an open pit mine selected as test site

Figure 3   High-resolution point clouds of two sectors of a wall of the open pit selected as test site

3   Methodology

3.1   Discontinuity extraction

The high-resolution point cloud collected during the field campaign has been processed in order to identify the main geological structures daylighting on the bench faces. Specifically, a semi-automatic extraction of the main geomechanical characteristics of the rock mass discontinuities has been performed using a MATLAB tool called DiAna, which stands for discontinuity analysis (Gigli & Casagli 2011), deriving information about the geometric parameters of the discontinuities such as orientation, number of sets, persistence, etc.

The analysis has been carried out in correspondence of each geotechnical domain identified in the analysed sector of the pit, as shown in Figure 4.

The identified discontinuities have been validated through a comparison with data acquired by photogrammetric surveys (Figure 4). The obtained structural data represent the input for the 3D kinematic analysis and the related generation of 3D maps of the kinematic hazard indexes for each possible instability mechanism.
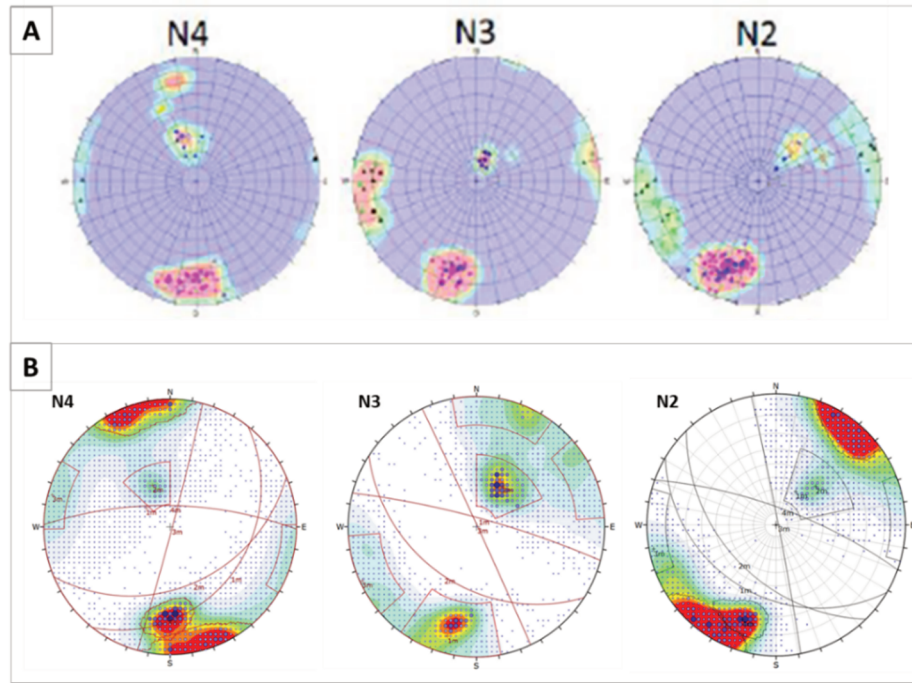

Figure 4   **(a) Stereoplots showing the discontinuities extracted by the geotechnical staff of the pit; (b) Stereoplots of the discontinuities extracted by applying the proposed procedure, in correspondence of the three structural domains identified as N4, N3 and N2, within the analysed wall of the pit**

3.2   Kinematic analysis

The kinematic analysis can provide information about the possible occurrence of instability events related to kinematically feasible mechanisms, given the geometry of the slope and discontinuities.

Specifically, a map of the distribution of the kinematic hazard index within the investigated area for each possible instability mechanism, such as plane failure (PF), wedge failure (WF), flexural toppling (FT) and block toppling (BT), is given. These indexes (C_{pf}, C_{wf}, C_{ft} and C_{bt}) are calculated by counting poles and discontinuities falling into discrete critical areas, which satisfy specific failure conditions, as indicated in Figure 5.

Planar failure: $C_{pf} = \dfrac{N_{pf}}{N}$ (%)

Wedge failure $C_{wf} = \dfrac{I_{wf}}{I}$ (%)

Flexural toppling $C_{ft} = \dfrac{N_{ft}}{N}$ (%)

Block toppling $C_{bt} = \dfrac{N_{bt}}{N} \dfrac{I_{bt}}{I}$ (%)

N= number of poles satisfying a specific failure condition;
I = number of intersections satisfying a specific failure condition

Figure 5   Kinematic indexes as defined by Casagli & Pini (1993)

The kinematic conditions necessary to generate structurally controlled failures are schematised in Figure 6.
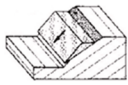
MECHANISM	CONDITIONS FOR KINEMATIC ADMISSIBILITY	
Plane Failure (PF)	$\alpha_d = \alpha_s \pm 20°$ α_d: dip direction of the discontinuity plane; α_s: dipe direction of the bench face.	$\phi < \beta_d < \beta_s$ β_d: dip of the discontinuity plane; β_s: dip of the bench face; Φ: friction angle.
Wedge Failure (WF)	Wedge on both planes: if the dip direction of two planes lie outside the included angle between α_i* and α_s**; Wedge on only one plane: if the dip direction of the one plane lies within the included angle between α_i* and α_s**, the wedge will slide on only that plane. $*\alpha_i$: dip direction of the intersection plane; $**\alpha_s$: dip direction of the bench face.	$\phi < \beta_i < \beta_s$ β_i: dip of the intersection line; β_s: dip of the bench face; Φ: friction angle.
Block Toppling (BT)	$\alpha_d = \alpha_s \pm 20°$ (except for very steep slope faces) α_d: dip direction of the discontinuity plane; α_s: dip direction of the bench face.	$\beta_{d(basal\ plane)} < \beta_s$ $\beta_{d(basal\ plane)} < \phi$ β_d: dip of the discontinuity plane; β_s: dip of the bench face; Φ: friction angle.
Flexural Toppling (FT)	$\alpha_d = \alpha_s \pm 10°$ α_d: dip direction of the discontinuity plane; α_s: dip direction of the bench face.	$(90° - \beta_s) + \phi < \beta_d$ β_d: dip of the discontinuity plane; β_s: dip of the bench face; Φ: friction angle.

Figure 6 Kinematic conditions for structurally controlled failures occurrence (αd = discontinuity dip direction, αs = slope dip direction, βd = discontinuity dip angle, βs = slope dip angle, φ = friction angle)

Applying the proposed methodology, a map for each kinematic hazard index has been obtained (Figure 7). These maps show the values of the kinematic index which range from 0% (none of the mapped discontinuities satisfies kinematic conditions for that part of the slope) to 100% (all the mapped discontinuities satisfy the kinematic conditions for that part of the slope).

The obtained 3D kinematic maps on the analysed wall of the pit identify planar and FT as the failure modes with the highest kinematic index, reaching maximum values of 30%. WF is also kinematically feasible but to a minor extent. The areas with the highest values of kinematic index are the east sector of analysed wall and the lower part of the slope.

From the 3D kinematic maps, it is also possible to derive a map showing the predominant mechanism in correspondence of each point of a laser cloud (for each point of the cloud the mechanism with the highest kinematic index is shown) (Figure 8).
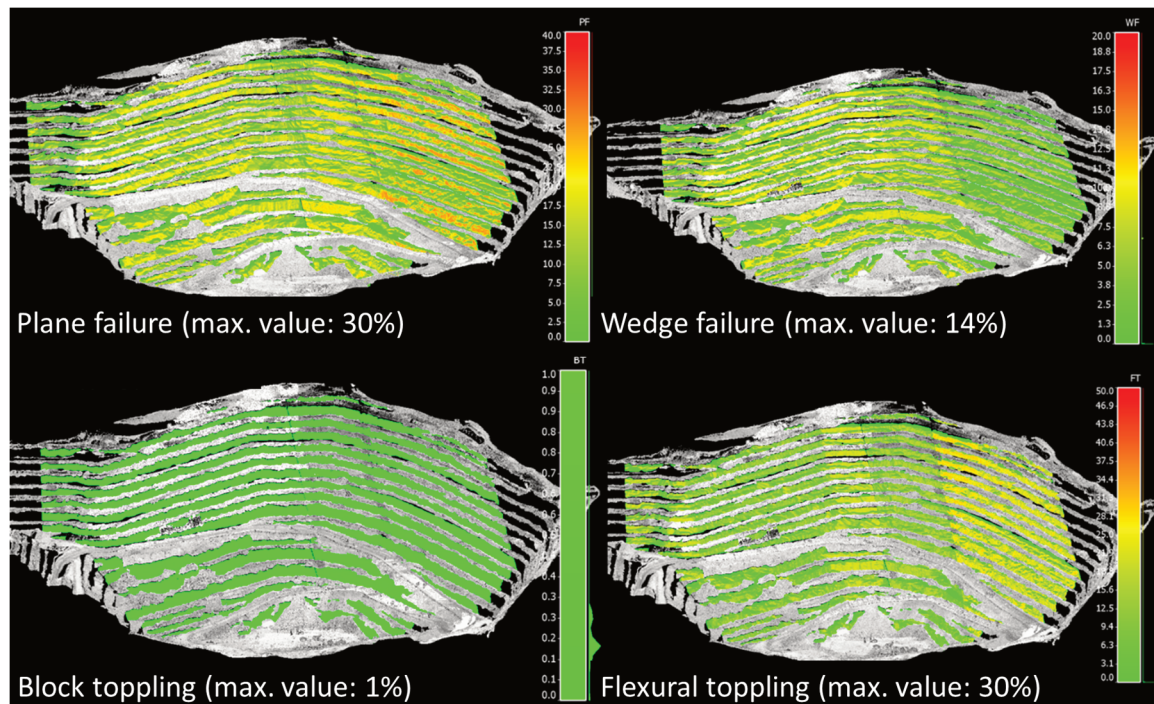
Figure 7   3D kinematic analysis identifying the sectors of the analysed slope more prone to the different possible failure mechanisms
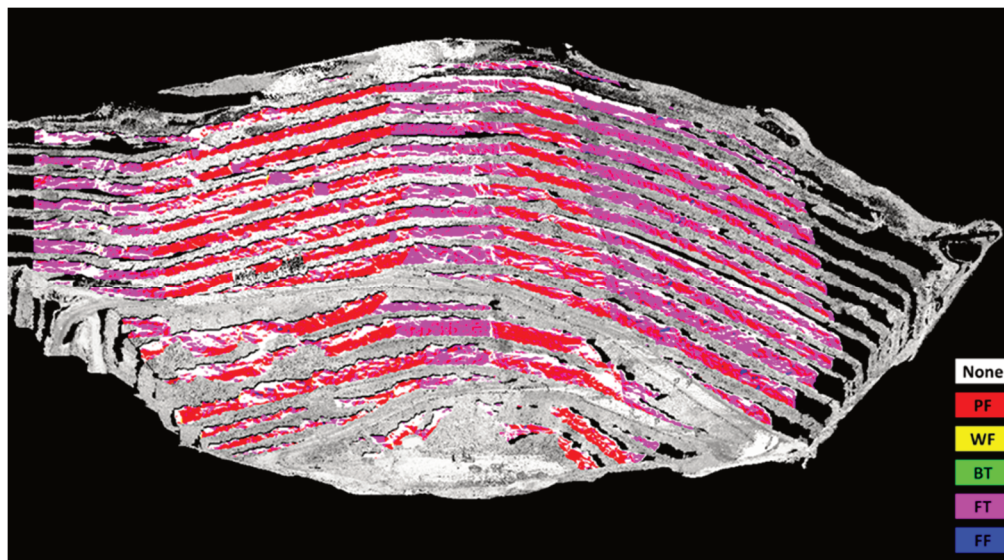

Figure 8   Map of the predominant failure mechanism (PF = planar failure, WF = wedge failure, BT = clock toppling, FT = flexural toppling, FF = free fall)

3.3   Correction of radar data

Once the main possible instability mechanisms have been identified, the direction of movement for each of them was estimated in terms of dip and dip direction by deriving it from the kinematic conditions to be satisfied in order to have kinematic feasible mechanisms.

Specifically, the following steps have been carried out:

1. Identification of the discontinuities (for PF and toppling) or the intersections between discontinuity planes (in case of WF), that can determine structurally-controlled instability events due to their intersection with the local topography (aspect and slope) (i.e. the output of the 3D kinematic analysis).

Combining structural data with monitoring data in open pit mines to interpret
the failure mechanism and calibrate radar alarms

P Farina et al.

2. Evaluation of the average value of the poles of the discontinuities, in correspondence of each point of the cloud, which satisfy the kinematic conditions related to the instability events (falling within the critical sector of the stereoplot for the considered mechanism).

3. Measurement of the dip and dip direction of the defined average pole, in correspondence of each point of the cloud.

The application of the proposed procedure to each point of the cloud allowed us to obtain maps of dip and dip direction of the estimated displacement direction for each failure mode. In Figure 9, the example of the expected direction of movement for the FT mechanism is reported. FT is a mode of failure involving the bending of interacting rock columns formed by a single set of steeply dipping discontinuities. Kinematic conditions necessary for the occurrence of a FT are summarised in Figure 10. Discontinuities must dip into the slope face. Dip direction of the discontinuities must be nearly parallel (±10◦) to the slope face to allow a series of slab parallel to the slope to form. The dip of the planes must be steep enough for interlayer slip to occur. Slip will occur only if the direction of the applied compressive stress is at angle greater than ϕ (friction angle of the faces between slabs). The direction of the major principal stress in the cut is parallel to the face of the cut (dip angle ψ_f), interlayer slip and toppling will occur only on planes with dip ψ_p, when $\psi_p > \phi + (90° - \psi_f)$.

The maps of dip and dip direction of each possible failure mechanism have been combined with the radar LOS information, obtaining maps showing the percentage of displacement effectively detectable by the radar system, due to its location, called sensitivity maps. In order to calculate the radar sensitivity, the radar LOS and the estimated direction of movement were considered as versors and the angle between the two versors were calculated by using their directional cosines. In fact, the absolute value of the cosine of the angle between two versors or two planes can be calculated as the scalar product between the two versors. The cosine of the angle between the radar LOS and the direction of movement represents the correction factor of the radar LOS to the actual direction of movement. Its inverse value is representative of the sensitivity of the radar LOS and it varies from 0% (movement direction perpendicular to radar LOS) to 100% (movement direction parallel to radar LOS).
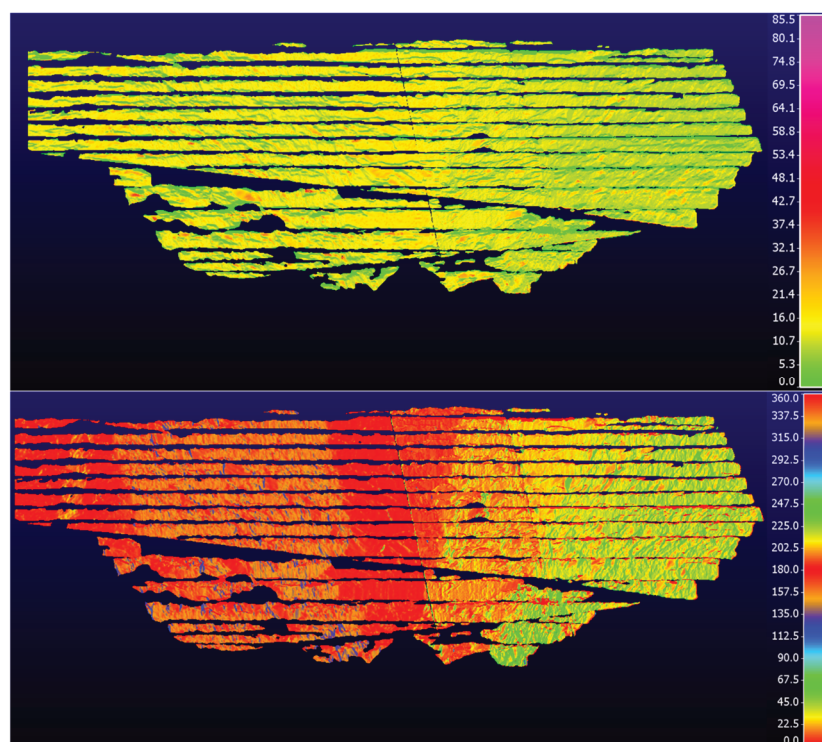

Figure 9   Maps with the dip and dip direction of the flexural toppling mechanism, on the analysed wall of the pit
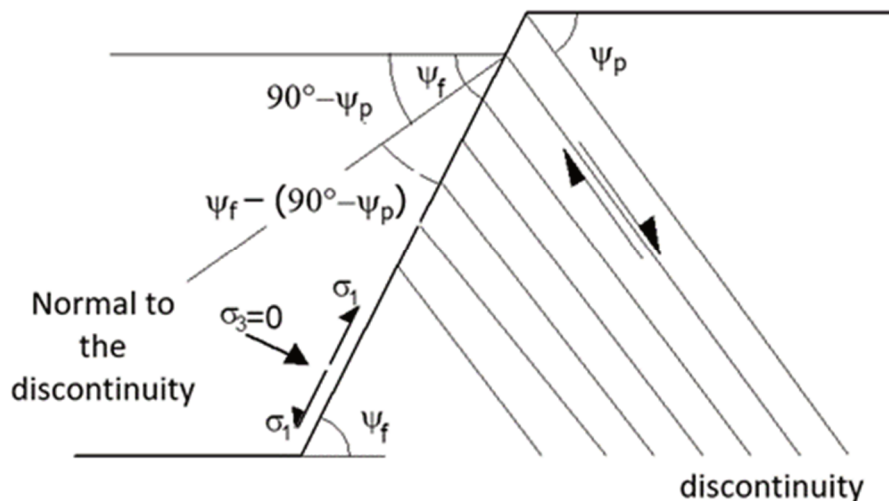
Figure 10   Kinematic conditions to be satisfied for the occurrence of flexural toppling

For the test site, the radar sensitivity to FT is generally high and near to 100% within the whole observed area, as can be observed from Figure 11. Localised areas, specifically at the bottom of the pit and in correspondence of the western sector, are characterised by lower sensitivity values.
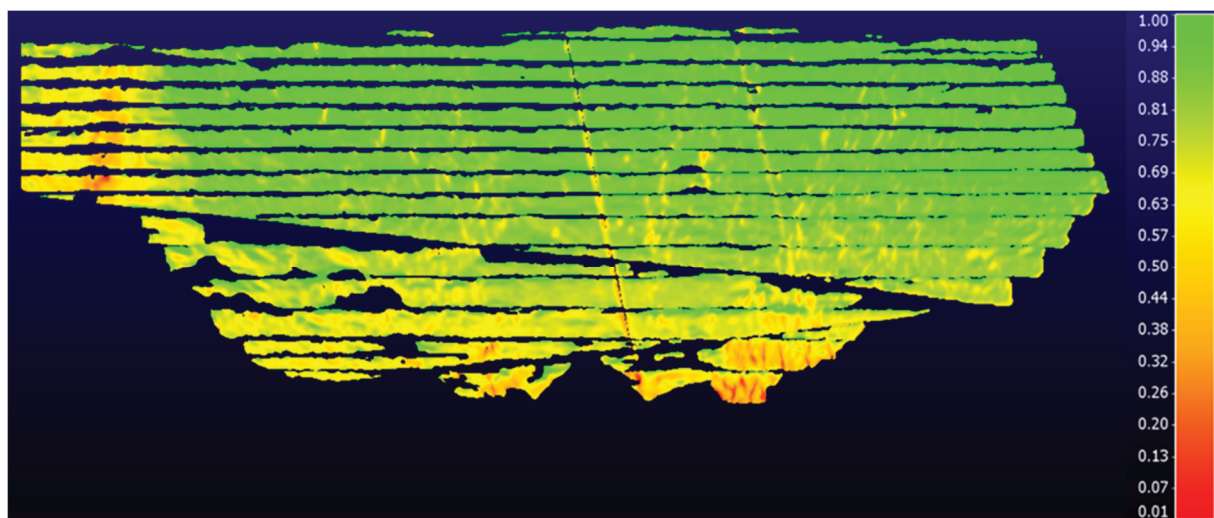

Figure 11   Map showing the radar sensitivity to the flexural toppling mechanism on the analysed area

The case shown in Figure 12 represents a 3D sketch of the relationship between the estimated displacement vector and the component detected by the radar system installed within the open pit. In the furnished example, the instability mechanism affecting the area has been classified as a FT based on the outcomes of the 3D kinematic analysis. Once the expected direction of movement is estimated from the proposed methodology and the radar sensitivity is calculated, it is possible to correct the radar measurements by multiplying the radar LOS data by the correction factor (inverse of the sensitivity). In Figure 13, an example of LOS radar displacement map, showing the deformations associated with a slope failure, and the corresponding corrected displacement map are shown.
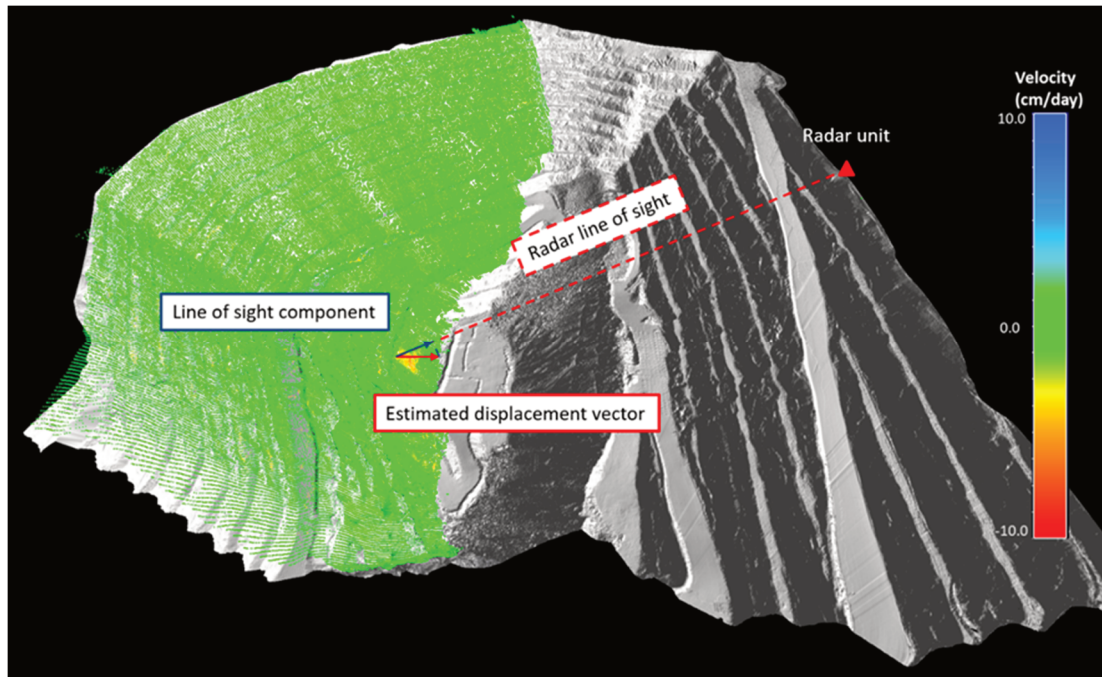
Combining structural data with monitoring data in open pit mines to interpret
the failure mechanism and calibrate radar alarms

P Farina et al.

Figure 12 Geometrical relation between real displacement vector and the component measured by the radar system visualised over the velocity map (coloured from green to red) obtained from the radar installed onsite
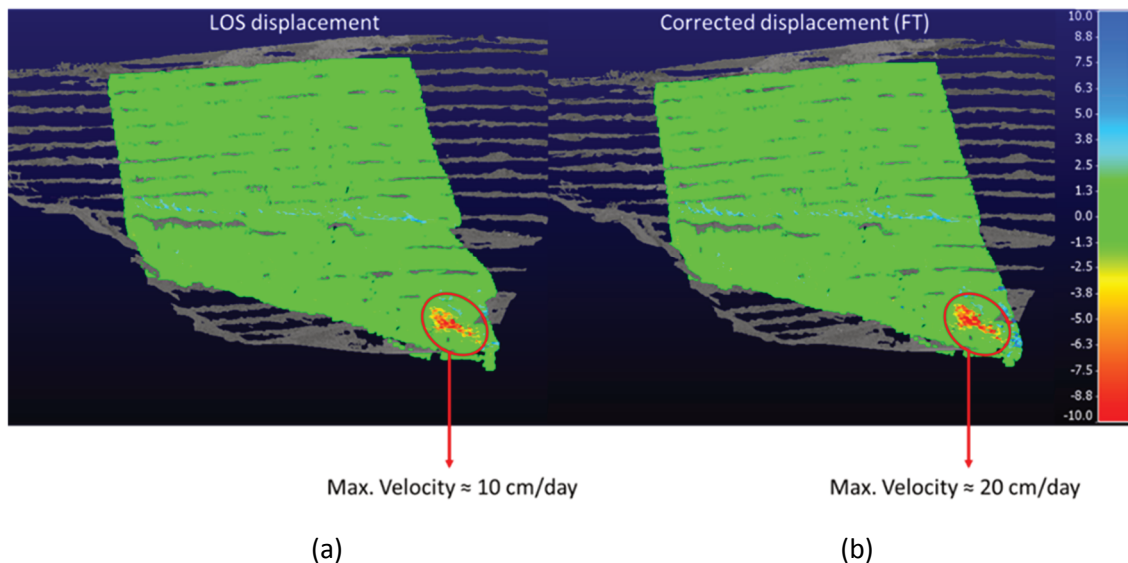

Figure 13 (a) LOS displacement and (b) corrected displacement of a failure event occurred on the analysed wall of the open pit mine

In the proposed example, the correction factor for such an area for what concern FT is around 2 (meaning that the sensitivity of the radar LOS to the expected direction of movement is 0.5). Therefore, the results of proposed approach suggest reducing by half the alarm thresholds proposed by the geotechnical team of the pit for this specific area located at the bottom of the slope.

In order to validate the proposed procedure, the estimated direction of the displacement was compared to the actual displacement direction detected by the robotic total station on the installed prisms on the wall of the analysed pit where a slope failure occurred (Figure 14). Figure 15 shows the 3D sketch where the displacement direction estimated from the proposed methodology was compared with the one inferred by the total station, in correspondence of a prism located near to the analysed failure.
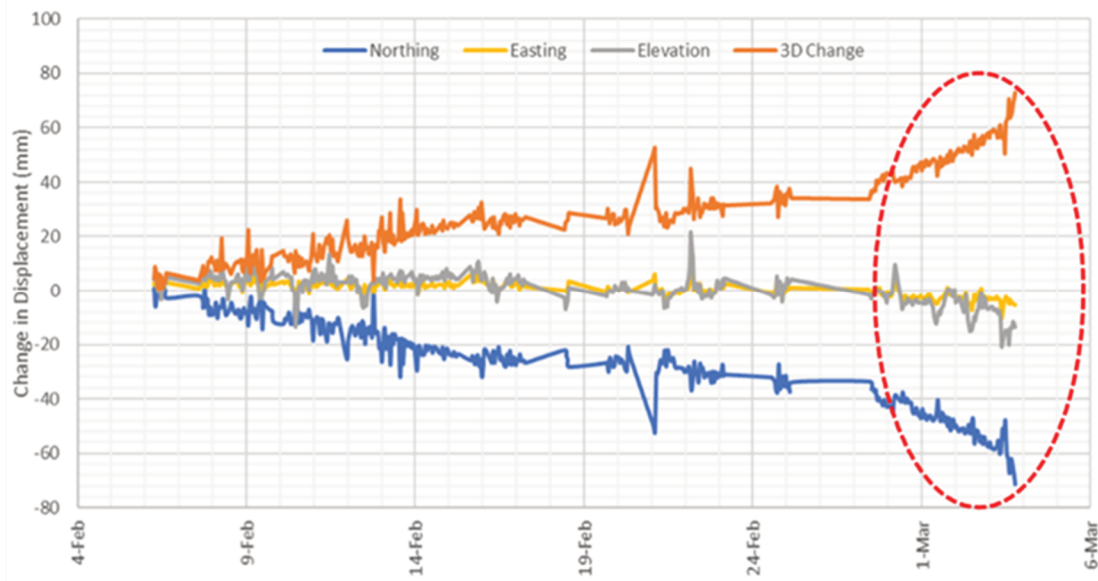
Figure 14 Northing, easting, elevation and 3D displacement obtained from a prism measured in a failure area
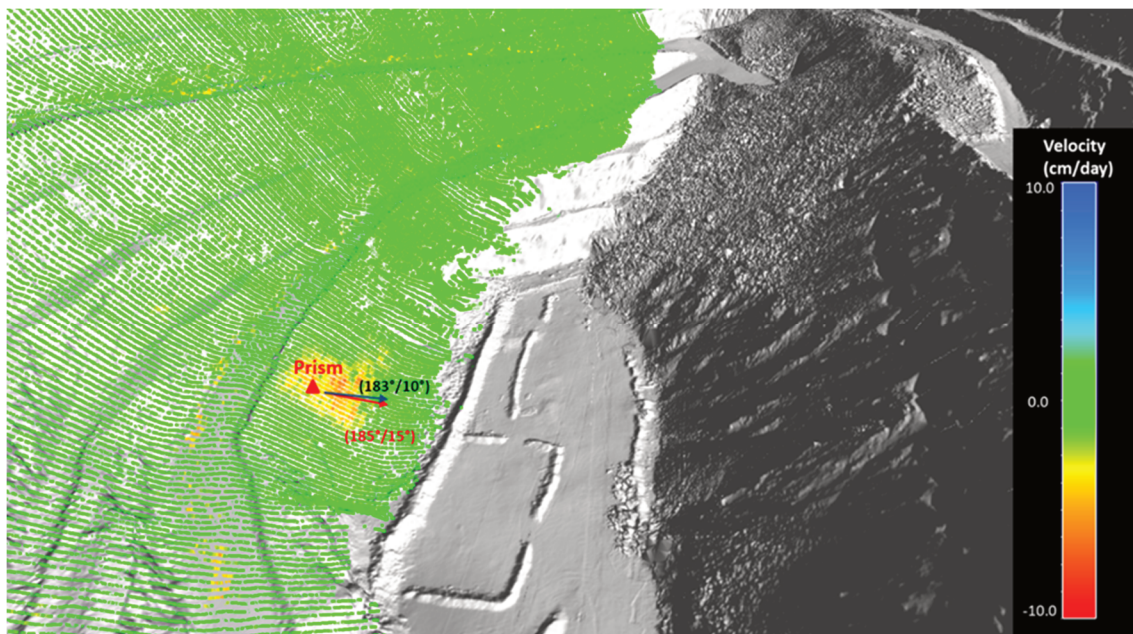

Figure 15 Example of validation procedure performed comparing the displacement vector direction estimated from the kinematic analysis (the blue arrow), with the direction of the displacement vector measured by total station (the red arrow)

4 Conclusions

The proposed method based on the quantitative combination of structural data, in the form of 3D kinematic index maps, with displacement records acquired by radar, represents an operational methodology to support the understanding of the relationship between observed deformations and structural stability controls. In addition, the output of the analysis is aimed at improving the effectiveness of the slope monitoring program thanks to the input provided to a better selection of alarm thresholds.

The main objective of this research was to develop a method to support geotechnical engineers in large open pits in the daily interpretation of slope monitoring data and in the set-up of alarm thresholds.

Combining structural data with monitoring data in open pit mines to interpret
the failure mechanism and calibrate radar alarms

P Farina et al.

By analysing high-resolution point clouds of sectors of open pits affected by failures, innovative algorithms have been applied to extract information about the main discontinuity sets of the study areas, and, according to the geometry of the discontinuities and their relative location respect to the slope orientation, deriving information about the possible occurrence of structurally controlled failure mechanisms. Hazard kinematic indexes related to the main possible instability mechanisms have been calculated in correspondence of each point of the clouds. These indexes vary from 0 (none of the mapped discontinuities satisfies kinematic conditions for that part of the slope) to 100% (all the mapped discontinuities satisfy the kinematic conditions for that part of the slope).

Thanks to the results of kinematic analysis, displacement direction–in terms of dip and dip direction–of each possible failure mechanism in correspondence of each portion of the slope, was estimated.

The results of 3D kinematic analysis represented a valuable tool to better interpret monitoring data acquired by slope stability radar. Taking into account the main characteristic of radar systems, which consists in the availability to acquire only the LOS component of displacement vector, the radar sensitivity to the estimated direction of movement, inferred from 3D kinematic analysis, was evaluated. Radar sensitivity information plays a key role in the calibration of radar alarms.

In order to validate the methodology, its results were compared with monitoring data acquired by robotic total station installed onsite, measuring 3D displacement of prisms located in correspondence of the analysed failure events.

Acknowledgement

References

Casagli, N & Pini, G 1993, 'Analisi cinematica della stabilità in versanti naturali e fronti di scavo in roccia' (Kinematic analysis of stability in natural slopes and rock excavation fronts), *Proceedings 3° Convegno Nazionale dei Giovani Ricercatori in Geologia Applicata* (Proceedings of the 3rd National Conference of Young Researchers in Applied Geology), L'Associazione Italiana di Geologia Applicata e Ambientale, Pavia.

Gigli, G & Casagli, N 2011, 'Semi-automatic extraction of rock mass structural data from high resolution LIDAR point clouds', *International Journal of Rock Mechanics and Mining Sciences*, vol. 48, no. 2, pp. 187–198.

Goodman, RE & Bray, JW 1976, 'Toppling of rock slopes,' *Proceedings of the Specialty Conference on Rock Engineering for Foundations and Slopes,* American Society of Civil Engineers, Boulder, vol. 2, pp. 201–234.

Hoek, E & Bray, JW 1981, *Rock Slope Engineering,* revised 3rd edn, CRC Press, London.

Hudson, JA & Harrison, JP 1997, *Engineering Rock Mechanics: An Introduction to the Principles*, Elsevier Science Ltd, Amsterdam.

Matheson, GD 1983, *Rock stability assessment in preliminary site investigations - Graphical Methods*, Transport and Road Research Laboratory, Wokingham.